Carbohydrate Polymers 87 (2012) 1787–1795

Contents lists available at SciVerse ScienceDirect

Carbohydrate Polymers

journal homepage: www.elsevier.com/locate/carbpol

Development of a phytochemical scaffold for bone tissue engineering using *Cissus quadrangularis* extract

S. Soumya [1], K.M. Sajesh [1], R. Jayakumar, S.V. Nair, K.P. Chennazhi *

Amrita Centre for Nanosciences and Molecular Medicine, Amrita Institute of Medical Sciences and Research Centre, Amrita Vishwa Vidyapeetham University, Kochi 682 041, India

ARTICLE INFO

Article history:
Received 16 August 2011
Received in revised form
26 September 2011
Accepted 30 September 2011
Available online 6 October 2011

Keywords:
Bone tissue engineering
Herbal scaffold
Cissus quadrangularis
Alginate
O-Carboxymethyl chitosan
hMSCs

ABSTRACT

A novel "herbal scaffold" (Alg/*O*-CMC/CQ-E scaffold) was fabricated by incorporating medicinal plant *Cissus quadrangularis* (*CQ*) *extract* with natural biopolymers alginate (Alg) and *O*-carboxymethyl chitosan (*O*-CMC) by lyophilization technique The prepared composite scaffolds were characterized using scanning electron microscopy (SEM), Fourier transform infrared spectroscopy (FTIR) and X-ray diffraction analysis (XRD). Preliminary cytocompatibility studies with human mesenchymal stem cells (hMSCs) supports the biocompatible nature of the composite scaffolds. There was a significant difference in initial cell attachment and proliferation on the herbal scaffolds compared to scaffolds fabricated without extract. Moreover, the hybrid scaffold favoured a substantially enhanced differentiation of hMSCs to osteoblasts, even without osteogenic media supplements, followed by increased calcified mineral deposition within two weeks of incubation. Hence, our primary investigation of physico-chemical and biological properties of the herbal scaffolds suggests that this osteoinductive scaffold could serve as a potential candidate for bone tissue engineering therapeutics.

1. Introduction

Tissue engineering is considered to be the most innovative biomedical methodology in the restoration and repair of defective and damaged tissues, by focusing on the regeneration of neotissues from cells with the support of biomaterials and growth factors. For bone regeneration, different biomaterials are currently being used which not only serves as a substrate for seeded cells but also supports the formation of new matrix deposition (Kneser, Schaefer, Polykandriotis, & Horch, 2006). Ideally, the scaffolds for bone tissue engineering should provide high structural integrity, high surface area for cell–material interaction and slow degradation at a rate which commensurate with the elucidation of new bone tissue formation (Joshua, Timothy, & Ketul, 2009). Moreover, the mechanical properties of the scaffolds should also match up with moduli of bone since it has to transmit mechanical forces and manage mineralization requirements (Vunjak-Novakovic & Goldstein, 2005). However, though the currently available biomaterials are known for their good biocompatibility and mechanical properties, they do not possess the necessary bioactivity properties for good tissue regeneration, i.e. not only the osteoconductive properties but also osteoinductive properties.

The osteogenic cells derived from mesenchymal or stromal stem cells uniquely elaborate the matrix of bone. These cells differentiate into mature osteoblasts, which then actively synthesize and mineralize bone matrix (Harada & Rodan, 2003). The development of agents that possess osteogenic activity will enhance the above process. In the perspective of utilization of biologically active natural osteogenic agents, the plant species possessing medicinal properties that are being used in the ancient medicines are gaining much scrutiny of researchers. *Cissus quadrangularis* is one such medicinal plant possessing osteogenic activity and is attaining increasing interest as a potential therapeutic agent for enhancing bone healing. The pharmacological and therapeutic ability of *Cissus quadrangularis* is well studied (Garima, Saurabh, & Nagori, 2010; Jakikasem, Limsiriwong, Kajsongkarm, & Sontorntanasart, 2000). This plant has been customarily used in the bone fracture healing and also known as bonesetter for its ability to join bones (Potu et al., 2008; Chopra, Patel, Gupta, & Datta, 1975; Udupa & Prasad, 1964). Moreover, the extracts of this plant are reported to contain phytoestrogenic steroids, ascorbic acid, carotene, calcium and anabolic steroids (Madan, 1959; Mehta, Kaur, & Bhutani, 2001). The effects of *Cissus quadrangularis* on the bone marrow mesenchymal stem cell proliferation and osteogenic differentiation were also studied (Boisseson et al., 2004; Potu et al., 2009). Several previous *in vivo* experiments have demonstrated that CQ promotes ALP activity

Abbreviations: Alg, alginate; *O*-CMC, *O*-carboxymethyl chitosan; CQ, *Cissus quadrangularis*; CQ-E, *Cissus quadrangularis* extract.

* Corresponding author. Tel.: +91 484 2801234; fax: +91 484 2802020.
E-mail addresses: kpc619@gmail.com, drkrishnaprasadc@aims.amrita.edu (K.P. Chennazhi).

[1] These authors contributed equally.

0144-8617/$ – see front matter © 2011 Elsevier Ltd. All rights reserved.
doi:10.1016/j.carbpol.2011.09.094

and enhances collagen synthesis in the fracture-healing process (Shirwaiker, Khan, & Malini, 2003).

From this viewpoint, we report here for the first time an herbal scaffolding approach for bone tissue engineering applications where the extract of CQ was blended successfully with alginate and *O*-CMC. Alginate is a negatively charged nontoxic immunologically inert hydrogel, which have potential application in regeneration of many types of tissues (Vunjak-Novakovic et al., 2008; Mohan & Prabha, 2005). The carboxylic acid on alginate makes it attractive for modification. It undergoes ionotropic gelation in the presence of divalent cations (Honghe, 1997). Alginate is also known to breakdown to simpler glucose type residues, which is totally absorbable (Yoshito, 2006). In a recent report comparing the performance of various matrices, sodium alginate was shown to be an efficacious scaffold when used in the surgical construction of a prevascularised bone graft (Vogelin et al., 2002). Alginate has also been combined with other materials to enhance its biological performance such as with chitosan. Here, we have utilized *O*-carboxy methyl chitosan (*O*-CMC), which is a carboxy methyl derivative of chitosan. *O*-CMC is water-soluble and possesses many unique properties, such as biocompatibility, biodegradability, hydrophilicity and adsorption capability (Chen & Park, 2003; Fernando & Serigo, 2004). Through chemical crosslinking using $CaCl_2$ we could obtain a 3-D hydrophilic 'herbal scaffold' that retained microporous geometry. For in vitro assessment, human mesenchymal stem cells isolated from umbilical cord blood were chosen as a cell model for cell adhesion, proliferation as well as mineralization studies on Alg/*O*-CMC and Alg/*O*-CMC/CQ-E scaffolds.

2. Materials and methods

2.1. Materials

The *Cissus quadrangularis* plant was collected from Palakkad district of Kerala, India. Sodium alginate and $CaCl_2$ was purchased from Sigma–Aldrich. *O*-CMC was purchased from Koyo Chemicals Ltd., Japan. Hen lysozyme was purchased from Fluka. DAPI, Alamar blue, Fetal Bovine Serum (FBS) and Trypsin-EDTA were purchased from Gibco, Invitrogen. hMSC culture media used was Mesencult from Stem cell Technologies.

2.2. Preparation of alginate/O-CMC/CQ-E scaffold

The plant stem was cut into small pieces and shade dried. 10 g of the fine powdered plant material was soaked in 50 ml of 95% ethanol and stirred for 5 h and filtered using 0.22 μm syringe filtered. 10 ml of 2% alginate solution was mixed with 10 ml of 2% *O*-CMC solution with vigorous stirring. To this alginate/*O*-CMC mixture, 10 ml of the CQ extract was carefully added while stirring and kept for 10 min vortexing for complete mixing of solution. The solution was then frozen at −20 °C for 24 h and was subsequently lyophilized in a freeze drier (Christ Alpha 2–4 LD Plus) for 48 h. The freeze-dried samples were cut into equal parts and crosslinked with 1% $CaCl_2$ solution for 2 h. The scaffolds were further washed with distilled water and kept at −20 °C for 24 h and again lyophilized for 24 h. Fig. 1 represents the schematic representation of the Alg/*O*-CMC/CQ-E scaffold preparation.

2.3. Characterization

2.3.1. SEM

The morphology of the scaffold, cell attachment and mineral production by osteoblast were investigated by scanning electron microscopy (JEOLJSM-6490LA). For cell attachment studies, cells were fixed using 2.5% gluteraldehyde for 1 h at room temperature. Cells were dehydrated through the graded ethanol series from 50, 70, 90 to 100%. Scaffolds were then mounted on aluminium stubs and coated with ultra thin layer of Platinum.

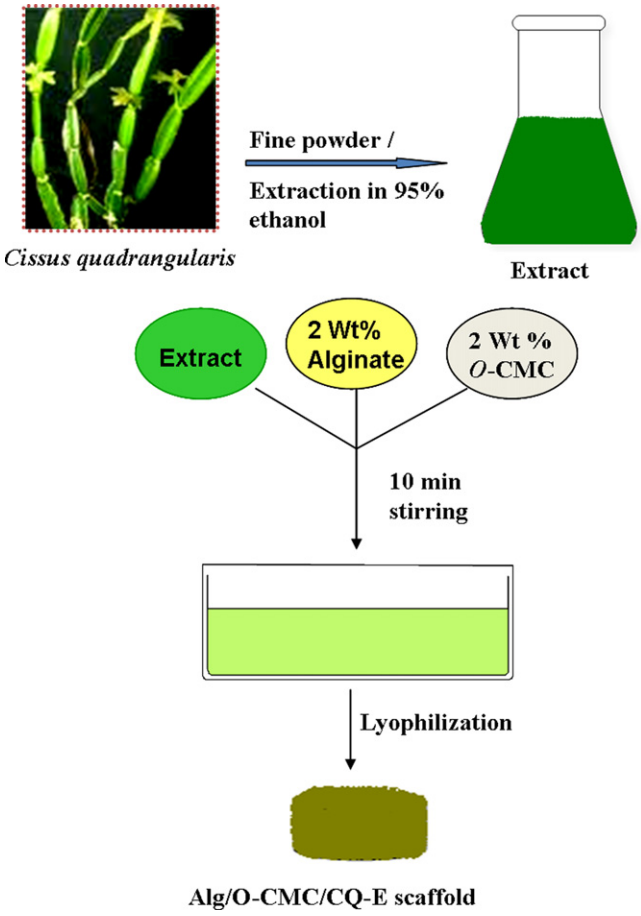

Fig. 1. The schematic representation of the Alg/*O*-CMC/CQ-E scaffold preparation.

2.3.2. FTIR

FTIR spectrum of Alg/*O*-CMC/CQ-E scaffold, Alginate, *O*-CMC and CQ extract were studied using Perkin Elmer Spectrum RX1 Fourier transform infrared spectrometer using the KBr method. The spectral analysis was carried out in the range of 400–4000 cm^{-1}. The biomineralization of hMSCs on the scaffold were also analysed using the FTIR data.

2.3.3. XRD

The mineral components of the plant extract was analysed using the XRD spectrum (PANalytical X'Pert-Pro). The extract was made into a thin film and analysed. Mineralization of the scaffold by the osteoblasts was also confirmed by the XRD spectral analysis. A thin layer of the scaffold after the mineralization process was taken for the analysis.

2.3.4. TGA

Thermal decomposition temperature measurement was carried out in simultaneous TGA–DTA instrument (SII TG/DTA6200) under nitrogen atmosphere using about 4 mg samples with a heating rate of 20 °C/min from room temperature to 500 °C.

2.4. Swelling studies

The medium uptake ability of the scaffold was studied in order to understand the diffusion of medium and nutrients into the scaffold. Previously weighed scaffolds were immersed in PBS at 37 °C

for a time period of 21 days. The wet weight of the scaffolds was measured in the time interval of 1, 3, 7, 14 and 21 days. The swelling ratio of the scaffolds in the respective days was calculated using the formula

$$\text{Swelling ratio} = \frac{\text{wet weight} - \text{dry weight}}{\text{dry weight}}$$

2.5. Porosity studies

The porosity of the scaffolds was measured using the liquid displacement technique (Zhang and Zhang, 2001). The scaffolds were immersed into the dehydrated alcohol for 48 h until it was saturated, and the porosity of the sample was calculated according to the formula

$$\text{Porosity} = \frac{\text{wet weight} - \text{dry weight}}{\text{density} \times \text{volume}} \times 100$$

2.6. Protein adsorption studies

Protein adsorptions on the Alg/*O*-CMC/CQ-E scaffold were estimated and compared with that of the control Alg/*O*-CMC using Bicinchoninic acid Assay (BCA). Complete Mesencult medium (Stem cell technologies) containing 10% Fetal Bovine Serum (Gibco, Invitrogen, USA) was used as a reference in this study. 500 μl of the complete medium was pipetted onto the scaffold kept in a 12-well cell culture plate. The scaffolds were then placed in a sterile humidified incubator at 37 °C for 6 h. Scaffolds were then washed twice with PBS to remove the unattached proteins. Samples were then kept for elution of adsorbed proteins in an elution buffer (0.5%CHAPS+ 0.025%SDS (Sigma Aldrich, USA) for overnight. After elution, total serum proteins adsorbed were quantified using BCA assay (Sigma Aldrich). Eluted samples were mixed with BCA reagent in the ratio 1:10 and incubated for 30 min and the optical density (OD) of the solution was measured at a wavelength of 562 nm using a microplate spectrophotometer (Biotek PowerWave XS, Highland Park, Winooski, VT). The concentration of adsorbed proteins was calculated from a concurrently produced standard curve with bovine serum albumin (BSA, Sigma Aldrich).

2.7. In vitro degradation studies

In order to determine the degradation of the Alg/*O*-CMC/CQ-E scaffold under the physiological conditions, the weight changes were analysed for a period of 28 days. The initial weights of the scaffold were noted and placed in 10 ml of PBS + lysozyme at 37 °C in a shaking incubator for a time period of 7, 14, 21 and 28 days. After the specified time, the scaffolds were washed with deionised water in order to remove the ions on the scaffold surface and were then freeze dried. The percentage degradation was calculated using the formula

$$\%\text{degradation} = \frac{\text{Initial weight} - \text{Dry weight}}{\text{Initial weight}} \times 100$$

2.8. Cell attachment studies

The adhesion and spreading of hMSCs on the scaffolds were analysed by SEM. The scaffolds were sterilized using ethylene oxide. The cells were seeded on the scaffold surface and cultured for 24 h. Following the incubation, cells were fixed using 2.5% gluteraldehyde for 1 h and the samples were dehydrated in graded ethanol series and were observed under SEM.

2.9. Cell viability assay

The viability of hMSCs on the scaffold was tested using Alamar blue assay. The scaffolds for the cell culture were sterilized using ethylene oxide gas in a standard ethylene oxide sterilization apparatus. hMSCs were seeded (10,000 cells/cm^2) onto the scaffold and cultured for 72 h. Following the incubation period, 10% of Alamar blue was added and kept for 4 h incubation. Subsequently after the incubation, 100 μl of medium from each sample was transferred to a 96 well plate and the absorbance of the solution was measured at 570 nm using a microplate reader (Biotek Power Wave XS), with 600 nm set as the reference wavelength.

2.10. Cell proliferation assay

The cell proliferation assay was carried out using Alamar blue test. The hMSC seeded scaffolds were incubated for 6 and 72 h. After the incubation, 10% Alamar blue solution was added and kept for 4 h incubation. The optical density of the solution was measured using Beckmann Coulter Elisa plate reader. Cell numbers were analysed from a concurrently plotted standard curve with hMSCs.

2.11. Analysis of hMSC differentiation by alkaline phosphatase (ALP) activity

The differentiation of hMSCs to ostoeblasts was assessed by measuring its ALP activity expression from 7 to 21 days. This assay relies on the ALP hydrolysis of p-nitrophenyl phosphate (Sigma) into a yellow product p-nitrophenol, the intensity of which was measured at 405 nm using an absorbance plate reader. Briefly, hMSCs were seeded onto the scaffolds at a density of 10,000 cells/cm^2. For measuring ALP activity, cells from 7, 14 and 21 days were taken and the cell lysate was prepared by treating the plates with 1% Triton-X-100 for 2 h at room temperature and subsequently sonicated for 20 min. After sonication, cellular debris was removed by centrifugation and aliquots of the cell lysates were collected for the analysis of ALP activity. ALP substrate was taken in a microtiter plate, and cell lysate was added to the substrate in a 1:1 ratio. After 30 min, 5 M sodium hydroxide (Sigma) was added to stop the enzymatic reaction. The OD of the reaction product was measured at 405 nm in the microplate spectrophotometer.

2.12. In vitro biomineralization studies

For the in vitro biomineralization studies, hMSCs were seeded onto the control as well as herbal scaffolds for a time period of two weeks in mesencult stem cell growth medium and the in vitro bio-mineralization by the cells were analysed using SEM, FTIR and XRD.

3. Results and discussion

3.1. Scaffold preparation

In an attempt to prepare an osteoinductive scaffold, the extract of the CQ was used. The loading amount was calculated as 10 mg/ml. Since there is no specific assay or spectroscopic method demonstrated for detecting the components in a crude plant extract, the release kinetics remains unanswered. The components in the plant extract were analysed using XRD spectra (Fig. 2A) and EDAX (Fig. 2B). The XRD spectrum clearly showed sharp intensity diffraction peaks at 24.5°, 30°, 38° and 46.5°, which confirmed the presence of calcium carbonate. The EDAX data also confirmed the presence of calcium, in the extract along with other components like phosphorous, potassium and magnesium. The lyophilized

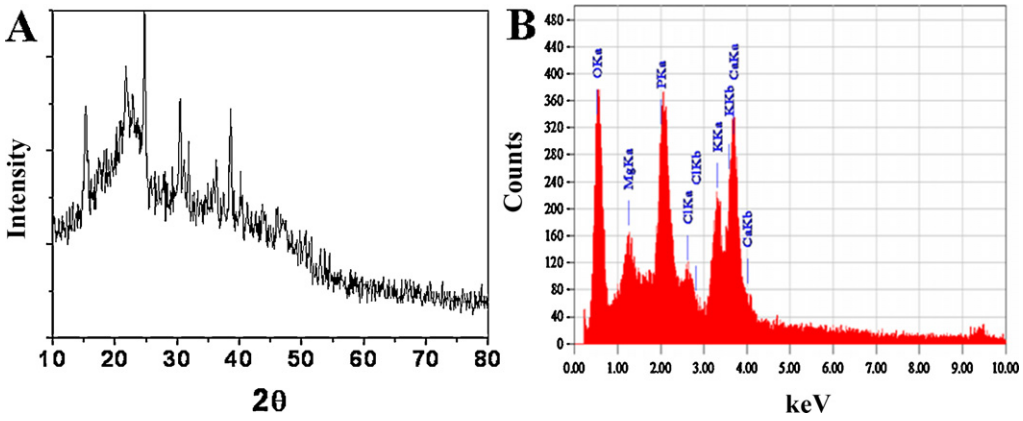

Fig. 2. (A) The XRD spectrum of CQ-E and (B) respective EDS spectrum of CQ-E.

extract as such is not suitable as a scaffold due to its weak mechanical stability. In order to improve the stability of the extract, cross linking with natural polymers like alginate, chitosan and modified chitosan were done in various concentrations ranging from 1 wt% to 3 wt%. $CaCl_2$ and gluteraldehyde were used as the cross linking agent in a range of concentrations from 0.1 to 2%. Among them, the 2% alginate solution mixed with 2% *O*-CMC solution along with the extract resulted in a better scaffold and is thus selected for subsequent studies.

3.2. Characterization of scaffold

The morphology of the prepared scaffolds was analysed using the scanning electron microscopy. Fig. 3A and B shows the SEM images of Alg/*O*-CMC/CQ-E and Alg/*O*-CMC scaffolds respectively. The 3-D pore structure of the Extract scaffold is evident from the image and is more porous than the scaffold without extract. This porous structure can very well facilitate the cell infiltration and its subsequent attachment. Several in vitro studies have shown that for bone tissue engineering, the material should possess well-controlled pore size and interconnections for optimal cell substrate interactions (Hutmacher, 2001).

FTIR spectral analysis of the samples was done to confirm the cross-linking mechanism. Alginate, *O*-CMC, CQ extract and Alg/*O*-CMC/CQ-E scaffolds were separately analysed and is depicted in Fig. 3C. The analysis showed the characteristic peak at 3400, 1614 and 1045 cm^{-1} attributed by the presence of –OH, >C=O, –CHOH groups of alginate. The respective peaks at 1734, 1251 and 890 cm^{-1} represent the stretching vibrational band of carbonyl, carboxyl and –NH groups of *O*-CMC. Cross-linking of the material was confirmed by a slight shift in the absorption peaks, particularly that of –COOH group of the alginate and the –OH group of the *O*-CMC. The scaffolds were cross-linked using 1% $CaCl_2$. The Ca^{2+} ions present in the extract also might have helped in the cross linking process. The Ca^{2+} ions ionically interact with –COO– groups of guluronic acid and mannuronic acid residues to form the cross-links (Honghe, 1997). The shift in absorption peak may be due to the ionic cross linking of –COOH groups. The broadening of peaks in the range of 3400–3500 cm^{-1} occurs due to the free –OH group. This indicates the possibility of cross-linking between the –COOH of alginate and –OH group of *O*-CMC.

The thermal stability of the Alg/*O*-CMC/CQ-E composite was analysed using TGA. Fig. 3D showed that the onset of decomposition of the scaffolds at about 60 °C. This could be attributed by the presence of water in the material. The second decomposition occurs at around 300 °C and this is could be due to the breaking of C–H bonds. From the results, it is clear that the thermal properties of the scaffold have not much changed due to the addition of extract.

3.3. Swelling ratio, porosity measurement and in vitro degradation of the scaffold

The medium uptake ability was performed to assess the absorbing capacity of the scaffold. The uptake of the medium was found out by calculating the swelling ratio of the scaffolds in the PBS. Swelling facilitates the filtration of cells into the scaffold. The swelling ratio was shown in Fig. 4A. From the obtained data, it is evident that the Alg/*O*-CMC/CQ-E scaffold shows considerable increase in the swelling ratio when compared to the scaffold without the extract. This can be attributed to the increased porosity of the scaffold by the addition of the extract and also due to the hydrophilic nature of the scaffold.

3.4. Porosity measurement

Porosity is of particular importance in bone tissue engineering because high rate of mass transfer is expected due to the metabolic characteristic of bone. The porosity of the scaffolds was measured by the liquid displacement method. From the analysis Fig. 4B the porosity of the Alg/*O*-CMC/CQ-E was found to be 78.42% and that of Alg/*O*-CMC scaffold was found to be 67.22%. Our results suggest that the addition of the extract causes the increase in porosity. When the extract is added into the Alg/*O*-CMC matrix, large numbers of extract particles get dispersed within the matrix. Upon freezing the solvent, particles get aggregated. During lyophilization, the solvent layer covered on the particle aggregates will get evaporated and thus form a porous structure. So the porosity of the scaffold increased with addition of the extract. Therefore, the Alg/*O*-CMC/CQ-E scaffold can be a suitable scaffold in the bone tissue engineering. Due to its higher porosity, the enhanced medium and nutrition flow to the seeded cells is possible and thereby increases the bone mineralization (Freed & Vunjak Novakovic, 1998).

3.5. In vitro degradation of the scaffold

In tissue engineering approach, the scaffold should ideally degrade as new tissue formation takes place (Langer and Vacanti, 1993). In order to substantiate the degradability of the Alg/*O*-CMC/CQ-E scaffold, the degradation study of the scaffold was done for 28 days in the PBS + lysozyme. The scaffolds were cross-linked with 1% $CaCl_2$. The scaffold cross-linked with 1% $CaCl_2$ got degraded up to 40% of its total weight after 28 days of incubation in

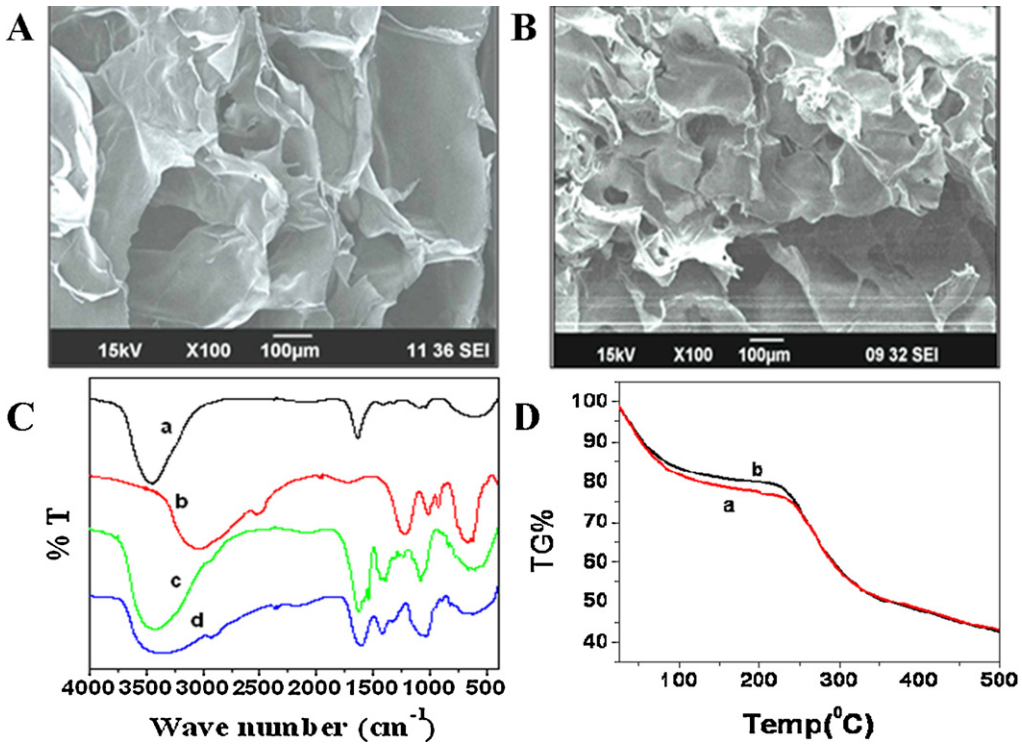

Fig. 3. (A) SEM image showing the morphology of Alg/*O*-CMC/CQ-E scaffold and (B) Alg/*O*-CMC scaffold. (C) FTIR spectrum of (a) alginate, (b) *O*-CMC, (c) extract and (d) Alg/*O*-CMC scaffold. (D) TGA data of the scaffolds (a) Alg/*O*-CMC/CQ-E scaffold and (b) Alg/*O*-CMC scaffold.

PBS + lysozyme as depicted in Fig. 4C. The lysozyme will cause the breakdown of gylcosidic linkage of CMC (Jayakumar et al., 2010). Therefore from the degradation studies, it can be concluded that the composite scaffold is degradable and has a structural stability in the physiological condition.

3.6. Protein adsorption studies

The protein adsorption property of the scaffolds was estimated by BCA assay. Protein adsorption is known to influence the cell adhesion by adsorption of key adhesion molecules like fibronectin

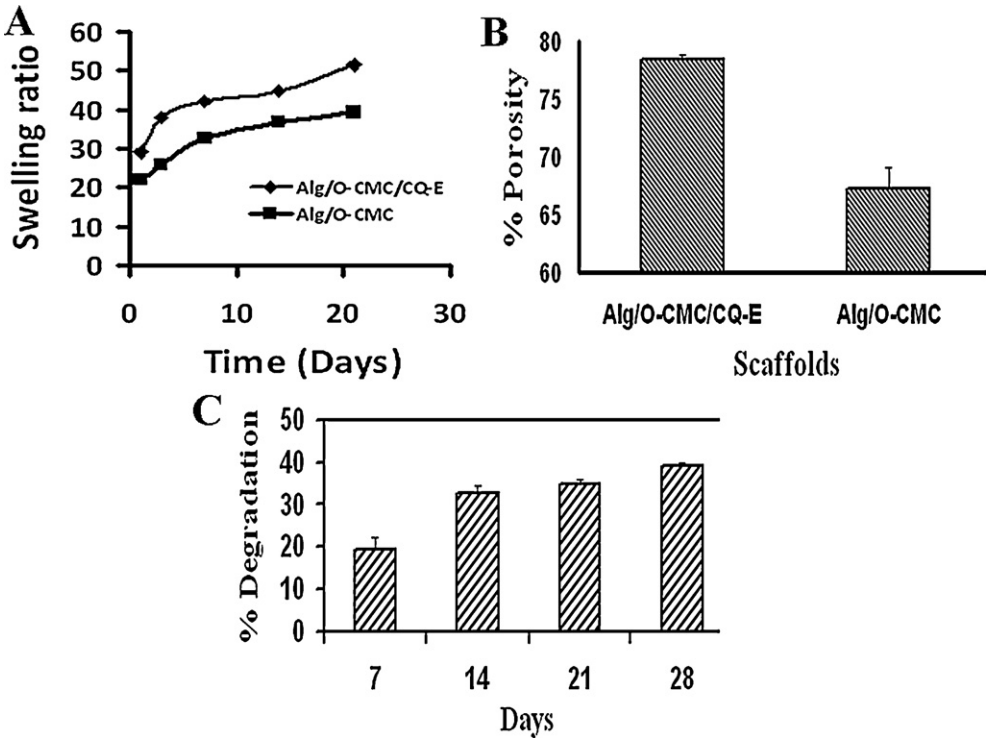

Fig. 4. (A) Swelling study of the scaffolds. (B) Porosity study of the scaffolds. (C) Degradation data of Alg/*O*-CMC/CQ-E scaffold cross-linked with 1% $CaCl_2$ for a period of 28 days.

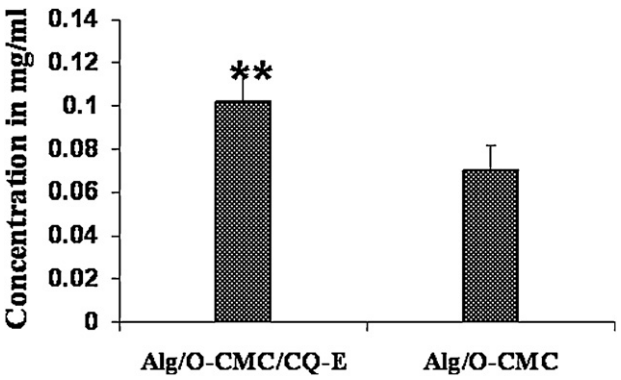

Fig. 5. Protein adsorption studies of the scaffolds; $^{**}p < 0.01$ for $n = 3$ samples.

or vitronectin (Kim, Kim, & Salih, 2005). The peptide bonds in protein reduce Cu^{2+} to Cu^{+}, which then chelates with Bicinichoninic acid and absorbs light at wavelength of 562 nm. The increase in protein adsorption of Alg/*O*-CMC/CQ-E scaffold when compared to the control is evident from Fig. 5. The presence of CQ-E imparted a superior surface property to the scaffold there by increased the binding sites for protein on the scaffold and promoted an electrostatic interaction between protein and scaffold surface.

3.7. Cell attachment studies

Cell attachment and distribution on the scaffolds were investigated by SEM. Fig. 6A and B shows the images of the cell attachment on alginate/O-CMC/Extract scaffold and alginate/*O*-CMC scaffold after 24 h in culture respectively. The cells on the Alg/*O*-CMC/CQ-E scaffolds appeared to be well-attached and well spread across the scaffold surface than the scaffolds without extract.

3.8. Cell viability assay and cell proliferation studies

The cell viability studies show that (Fig. 7A), there is not much difference in the cell viability of the Alg/*O*-CMC/CQ-E and Alg/*O*-CMC scaffolds. The Alginate and *O*-CMC are reported for its biocompatibility and has been used in several in vitro studies (Jayakumar et al., 2010; Klock et al., 1997). The incorporation of CQ-E into the scaffold enhanced its biocompatible property. Cell proliferation assay was analysed using the Alamar blue test. From the results (Fig. 7B), it can be inferred that the cell proliferation in the Alg/*O*-CMC/CQ-E and Alg/*O*-CMC scaffolds were in an extensive way and there is not much difference in both the cases at 6 h. But we can see after 72 h of culture period there is a marked difference in the cell proliferation on the Alg/*O*-CMC/E scaffolds than the scaffolds without extract. This could be due to the addition of the extract, which there by enhanced the cell proliferation.

3.9. ALP activity of hMSC on different matrices

Alkaline phosphatase (ALP) is an early marker for osteoblast differentiation. The ALP activity of hMSCs seeded on to the Alg/*O*-CMC/CQ-E shows a significant increase in the enzyme activity compared to the control Alg/*O*-CMC scaffolds (Fig. 8). At day 7, the ALP activity was roughly similar comparing the control scaffold. However, with by 14 days, ALP activity increased noticeably in the Alg/*O*-CMC/CQ-E scaffolds than the control Alg/*O*-CMC

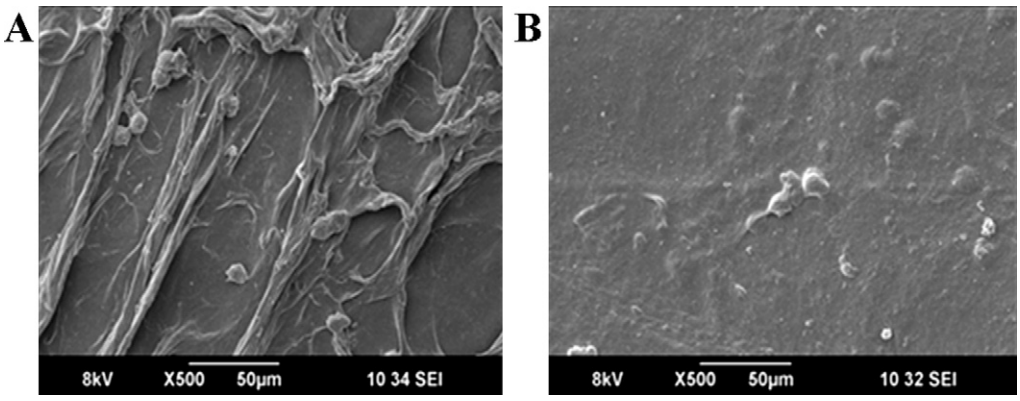

Fig. 6. SEM images showing the cell attachment on (A) Alg/*O*-CMC/CQ-E scaffold and (B) Alg/*O*-CMC scaffold.

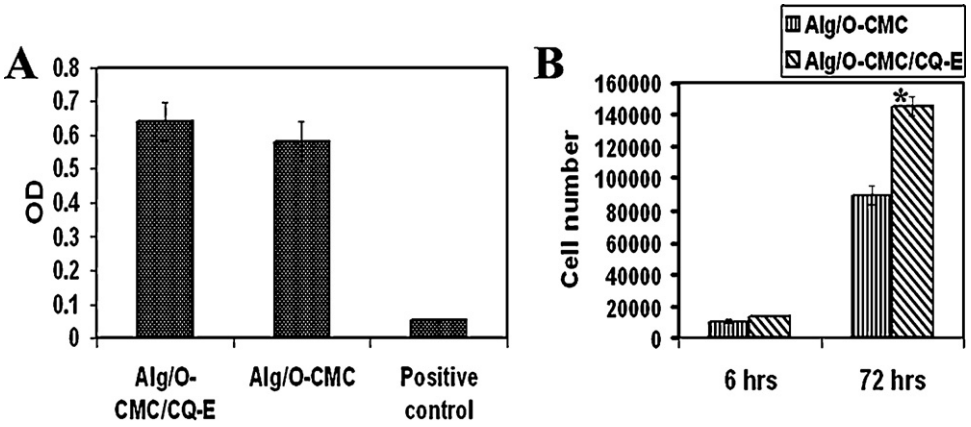

Fig. 7. (A) Showing cell viability studies of the scaffolds and (B) cell proliferation assay on the scaffolds by Alamar blue test. $^{*}p < 0.01$ for $n = 4$ samples.

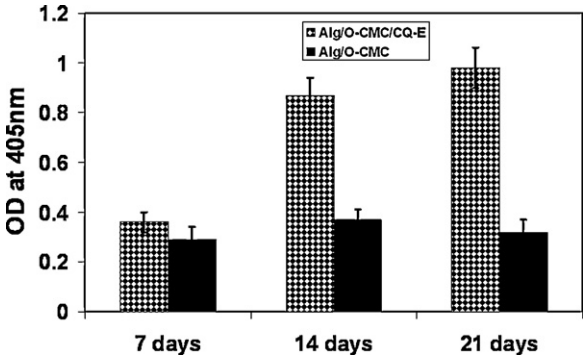

Fig. 8. Alkaline phosphatase activity of hMSCs on Alg/*O*-CMC/CQ-E scaffolds with the control Alg/*O*-CMC scaffolds over a period of 21 days. hMSCs on the Alg/*O*-CMC/CQ-E scaffolds showed significant increase in the enzyme activity over time than the control. $^{*}p < 0.01$ for $n = 5$ samples.

scaffolds. The increased ALP activity could be from the differentiated osteoblast cells growing within the functionalized scaffold. The fact that this happened without osteogenic media supplements illustrates the potential of herbal extracts in inducing differentiation of hMSCs into osteoblasts.

3.10. *In vitro* biomineralization studies

The final stage of hMSC differentiation to osteoblast is characterized by the formation of calcium phosphate nodules. The mineral deposition by the osteoblast cells were analysed by scanning electron microscopy. Fig. 9A–D shows the SEM images of mineralization on the Alg/*O*-CMC/CQ-E and Alg/*O*-CMC on 7 and 14 days respectively. The biomineralization ability of the osteoblasts derived from hMSCs on scaffolds for 14 days in culture revealed that the mineral deposition was significantly higher on scaffolds with extract than without CQ extract. This correlated well with the increased ALP activity observed by 14 days. The calcium phosphate

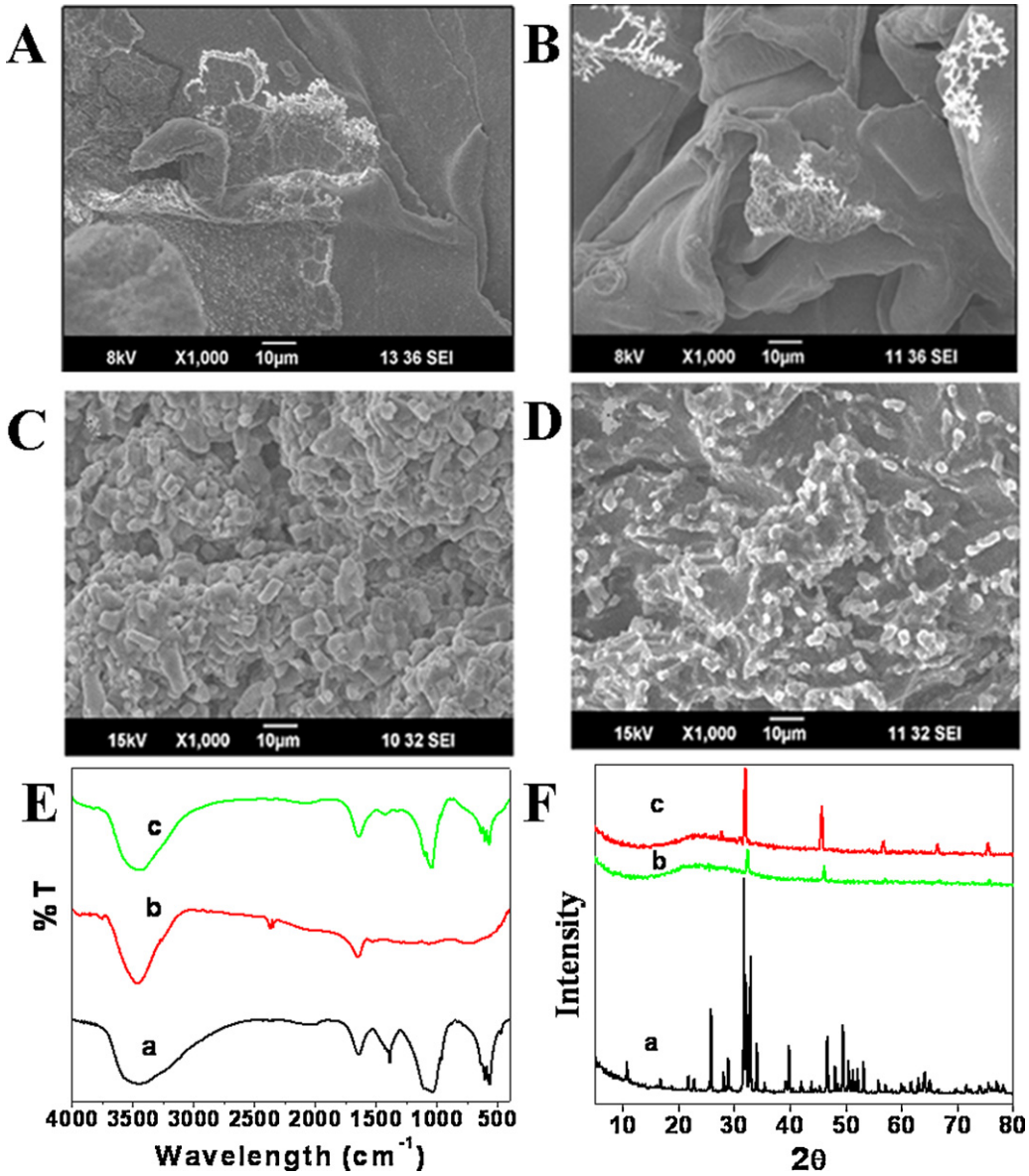

Fig. 9. SEM images showing the biomineralization of hMSCs grown on Alg/*O*-CMC/CQ-E and Alg/*O*-CMC analysed for 14 days. Left panel shows the biomineralization on Alg/*O*-CMC/CQ-E scaffold (A) 7th day and (C) 14th day; right panel shows the biomineralization of hMSCs on Alg/*O*-CMC; (B) 7th day, (D) 14th day. (E) FTIR spectrum of the mineralized Alg/*O*-CMC/CQ-E scaffold (a) HAp, (b) on day 7, (c) on day 14 and (F) XRD spectrum of the mineralized Alg/*O*-CMC/CQ-E scaffold (a) HAp, (b) on day 7, (c) on day 14.

deposition was confirmed using the XRD and FTIR spectrum. FTIR spectra depicted in Fig. 9E shows the corresponding peaks at 605, 660 and 3450 cm^{-1}, which are reported to be the characteristic peaks of HAp. The peak at 530 cm^{-1} corresponds to υ_4 PO_4 vibrations. The XRD studies Fig. 9F of the mineralized scaffold on the 14th day showed a sharp peak at 31.7° (2θ) attributed to (2 1 1) plane of hydroxyl apatite, which is the prominent mineral content of native bone (Madhumathi et al., 2009).

The osteogenic effect of *Cissus quadrangularis* has previously been suggested in number of *in vivo* studies. It is hypothesised that the CQ extract can accelerates the enzyme secretion by the osteoblasts, which accelerates the process of mineralization either by increasing the local concentration of inorganic phosphate or activating the collagen fibres to induce deposition of calcium salts (Udupa, Prasad, & Sen, 1965). Though its osteogenic activity has been suggested, the underlying mechanism still remains unclear. The phytogenic steroids found in CQ may be involved in stimulating osteoblastogenesis and may act on estrogen receptors of bone cells (Sen, 1963). The steroids can stimulate the proliferation and differentiation of osteoblasts and thereby increases the bone growth (Chagin, Chrysis, Takigawa, Ritzen, & Savendahl, 2006). The action of CQ on the enhanced mineralization of osteoblasts is likely mediated (Parisuthiman & Singhatanadgit, 2009; Prasad & Udupa, 1972). Also the anabolic steroidal principles show a marked influence in the rate of fracture healing by influencing early regeneration of all connective tissues involved in the healing and quicker mineralization of the callus (Shirwaiker et al., 2003). Our in vitro biomineralization results also support other researcher's findings that the presence of the phytosteroids in the extract could be one of the reasons for the increased mineralization of hMSCs on the herbal scaffolds compared to the scaffolds without extract.

4. Conclusions

In the present study, we have developed an osteoinductive 'herbal scaffold' with desirable properties requisite for a scaffold for bone tissue engineering applications. The active constituents of CQ extract, such as phytosteroids, enhanced the hMSC proliferation and promoted osteogenic differentiation and biomineralization process. Based on the above results it could be concluded that the Alg/*O*-CMC/CQ-E scaffold have excellent osteoinductive property, which along with the other desirable physico-chemical properties would make it an ideal candidate for bone tissue engineering. In the future perspective of this work, further experiments using the developed Alg/*O*-CMC/CQ-E scaffold is envisaged utilizing a flow-perfusion bioreactor providing different physiological stimulations necessary for bone regeneration.

Acknowledgements

The authors are thankful to Department of Science and Technology (DST), India for providing the financial support under the scheme of central grant of Nanoscience and Nanotechnology Initiative program monitored by Prof. C.N.R Rao. The authors are also grateful to Amrita Vishwa Vidyapeetham University for providing substantial infrastructure support for basic research in nanobiomedical sciences. Also we appreciate the help of Mr. Sajin P. Ravi and Sreeja V. Nair for the technical support in SEM and XRD analysis.

References

Boisseson, M. R., Leonard, M., Hubert, P., Marchal, P., Stequert, A., Castel, C., et al. (2004). Physical alginate hydrogels based on hydrophobic or dual hydrophobic/ionic interactions: Bead formation, structure, and stability. *Journal of Colloid and Interface Science*, *273*, 131–139.

Chagin, A. S., Chrysis, D., Takigawa, M., Ritzen, E. M. & Savendahl, L. (2006). Locally produced estrogen promotes fetal rat metatarsal bone growth: An effect mediated through increased chondrocytes proliferation and decreased apoptosis. *Journal of Endocrinology*, *188*, 193–203.

Chen, X. G. & Park, H. J. (2003). Chemical characteristics of *O*-carbobymethyl chitosan related to its preparation conditions. *Carbohydrate Polymers*, *53*, 335–359.

Chopra, S. S., Patel, M. R., Gupta, L. P. & Datta, I. C. (1975). Studies on *Cissus quadrangularis* in experimental fracture repair: Effect of chemical parameters in blood. *Indian Journal of Medical Research*, *63*, 824–828.

Fernando, R. D. A. & Serigo, P. C. (2004). Characterization and properties of carboxy methyl chitosan related to preparation conditions. *Carbohydrate Polymers*, *75*, 214–221.

Freed, L. E. & Vunjak Novakovic, G. (1998). Culture of organized cell communities. *Advanced Drug Delivery Reviews*, *33*, 15–30.

Garima, M., Saurabh, S. & Nagori, B. P. (2010). Pharmacological and therapeutic activity of *Cissus quadrangularis*: An overview. *International Journal of Pharm Tech Research*, *2*, 1298–1310.

Harada, S. & Rodan, G. A. (2003). Control of osteoblast function and regulation of bone mass. *Nature*, *423*, 349–355.

Honghe. (1997). Interaction mechanism in sol–gel transition of alginate solution by addition of divalent cations. *Carbohydrate Research*, *302*, 97–101.

Hutmacher, D. W. (2001). Scaffold design and fabrication technologies for engineering tissues-state of the art and future perspectives. *Journal of Biomaterial Science – Polymer Edition*, *12*, 107–124.

Jakikasem, S., Limsiriwong, P., Kajsongkarm, T. & Sontorntanasart, T. (2000). Phytochemical study of *Cissus quadrangularis*. *Thai Journal of Pharmaceutical Science*, *24*, 5.

Jayakumar, R., Prabaharan, M., Nair, S. V., Tokura, S., Tamura, H. & Selvamurugan, N. (2010). Novel carboxymethyl derivatives of chitin and chitosan materials and their biomedical applications. *Progress in Material Science*, *55*, 675–709.

Joshua, R. P., Timothy, T. & Ketul, C. P. (2009). Bone tissue engineering: A review in bone biomimetics and drug delivery strategies. *Biotechnology Progress*, *25*, 1539–1560.

Kim, H. W., Kim, H. E. & Salih, V. (2005). Stimulation of osteoblast responses to biomimetic nanocomposites of gelatin-hydroxyapatite for tissue engineering scaffolds. *Biomaterials*, *26*, 5221–5230.

Klock, G., Pfeffermann, A., Ryser, C., Grohn, P., Kuttler, B., Hahn, H., et al. (1997). Biocompatibility of mannuronic acid rich alginates. *Biomaterials*, *18*, 707.

Kneser, U., Schaefer, D. J., Polykandriotis, E. & Horch, R. E. (2006). Tissue engineering of bone: The reconstructive surgeon's point of view. *Journal of Cellular and Molecular Medicine*, *10*, 7–19.

Langer, R. & Vacanti, J. P. (1993). Tissue engineering. *Science*, *260*, 920–926.

Madan, N. (1959). Pharmalogical study of the stem of *Cissus quadrangularis* Linn. *Journal of Scientific and Industrial Research*, *18*, 253.

Madhumathi, K., Binulal, N. S., Nagahama, H., Tamura, H., Shalumon, K. T. & Selvamurugan, N. (2009). Preparation and charaterization of novel chitin–hydroxyapatite composite membranes for tissue engineering applications. *International Journal of Biological Macromolecules*, *44*, 1–5.

Mehta, M., Kaur, N. & Bhutani, K. (2001). Determination of marker constituents from *Cissus quadrangularis* Linn and their quantitation by HPTLC and HPLC. *Phytochemical Analysis*, *12*, 91–105.

Mohan, N. & Prabha, D. N. (2005). Novel porous, polysaccharide scaffolds for tissue engineering applications. *Trends in Biomaterial and artificial Organs*, *18*, 219–224.

Parisuthiman, D. & Singhatanadgit, W. (2009). *Cissus quadrangularis* extract enhances biomineralization through up-regulation of MAPK-dependent alkaline phoshatase activity in osteoblasts. *In Vitro Cellular and Developmental Biology – Animal*, *45*, 194–200.

Potu, B. K., Bhat, K. M. R., Rao, M. S., Nampurath, G. K., Chamallamudi, M. R., Nayak, S. R., et al. (2009). Petroleum ether extract of *Cissus quadrangularis* (Linn) enhances bone marrow mesenchymal stem cell proliferation and facilitates osteoblastogenesis. *Clinics*, *64*, 993–998.

Potu, B. K., Rao, M. S., Kutty, G. N., Bhat, M. R. K., Chamallamudi, M. R. & Nayak, S. R. (2008). Petroleum ether extract of *Cissus quadrangularis* (Linn) stimulates the growth of fetal bone during intrauterine developmental period: A morphometric analysis. *Clinic*, *63*, 815–820.

Prasad, G. C. & Udupa, K. N. (1972). Pathways and site of action of a phytogenic steroid from *Cissus quadrangularis*. *Indian Journal of Medical Research*, *4*, 132.

Sen, S. P. (1963). Preliminary clinical studies of *Cissus quadrangularis*. *Indian Journal of Medical Research*, *4*, 26.

Shirwaiker, A., Khan, S. & Malini, S. (2003). Antiosteoporotic activity of ethanol extract of *Cissus quadrangularis* Linn on ovariectomized rat. *Journal of Ethnopharmocology*, *89*, 245–250.

Udupa, K. N. & Prasad, G. C. (1964). Further studies on the effect of *Cissus quadrangularis* in accelerating fracture healing. *Indian Journal of Medical Research*, *52*, 26–35.

Udupa, K. N., Prasad, G. C. & Sen, S. P. (1965). The effect of phytogenic steroid in the accleration of fracture repair. *Life Science*, *4*, 317.

Vogelin, E., Jones, N. F., Lieberman, J. R., Baker, J. M., Tsingotjidou, A. S. & Brekke, J. H. (2002). Prefabrication of bone by use of a vascularized periosteal flap and bone morphogenetic protein. *Plastic and Reconstructive Surgery*, *109*, 190–198.

Vunjak-Novakovic, G., Fröhlich, M., Warren, L. G., Leo, Q., Marolt, D. & Drobni, M. (2008). Tissue engineered bone grafts: Biological requirements tissue

culture and clinical relevance. *Current Stem Cell Research and Therapy*, *3*, 254–264.

Vunjak-Novakovic, G. & Goldstein, S. A. (2005). In V. C. Mow, & R. Huiskes (Eds.), *Basic orthopaedic biomechanics and mechano-biology* (3rd ed., pp. 343–408). Philadelphia: Lippincott Williams and Wilkins.

Yoshito, I. (2006). Challenges in tissue engineering. *Journal of The Royal Society Interface*, *3*, 589–601.

Zhang, Y. & Zhang, M. (2001). Synthesis and characterization of macroporous chitosan/calcium phosphate composite scaffolds for tissue engineering. *Journal of Biomedical Material Research*, *55*, 304–312.